ISSN 1028-334X, Doklady Earth Sciences, 2023, Vol. 510, Part 1, pp. 262–268. © The Author(s), 2023. This article is an open access publication, corrected publication 2023.
ISSN 1028-334X, Doklady Earth Sciences, 2023. © The Author(s), 2023. This article is an open access publication.

GEOCHEMISTRY

Alkali Waters of the Ultrabasic Massif of Mount Soldatskaya, Kamchatka: Chemical and Isotopic Compositions, Mineralogy, and ^{14}C Age of Travertines

Yu. A. Taran[a], D. P. Savelyev[a,*], G. A. Palyanova[b], and Corresponding Member of the RAS B. G. Pokrovskii[c]

Received December 20, 2022; revised January 9, 2023; accepted January 16, 2023

Abstract—A detailed description of alkali water springs (pH > 10) found within the ultrabasic massif of Mount Soldatskaya in the Kamchatsky Mys Peninsula in Kamchatka is presented for the first time. The chemical composition of the springs and the dependence of the ratios and concentrations of some components on pH are indicative of the fact that these waters were involved in the present-day serpentinization of ultrabasic rocks. The springs with the highest alkali levels (pH 12.3) contain dissolved hydrogen at a concentration of about 0.6 mmol/l. The isotopic composition behavior of carbonate travertines deposited from these springs ($\delta^{13}C$ and $\delta^{18}O$) differs from the known trend of "meteogenic" travertines related to serpentinization of ultrabasic rocks in Oman and California. The age of travertines determined by the radiocarbon method is close to modern.

Keywords: alkali waters, Kamchatsky Mys Peninsula, ultrabasic rocks, serpentinization, age of travertine
DOI: 10.1134/S1028334X23600093

The formation of natural waters with pH > 11 has attracted the attention of many researchers over the past few decades, starting with Barnes et al. [1], due to the wide range of questions, problems, and applications that arise in the study of this natural phenomenon. In most cases, these waters originate from the present-day serpentinization of ultrabasic rocks. They are known both on the land, in a variety of tectonic settings, and on the seafloor, in mid-ocean ridges or fore-arc zones. The scientific and applied problems related to the formation of these waters range from the origin of abiogenic hydrocarbons and life, paleoclimatology, and chemical erosion to hydrogen energy and carbon dioxide sequestration. The extensive literature devoted to these problems can be found in a number of reviews and papers (for example, [2–4]).

The main chemical process leading to serpentinization of ultrabasic rock can be given in general as

$$\underset{\text{olivine}}{(Mg,Fe^{2+})_2SiO_4} + H_2O \Rightarrow \underset{\text{serpentine}}{Mg_3Si_2O_5(OH)_4} + \underset{\text{magnetite}}{Fe_3O_4} + H_2. \quad (1)$$

In fact, this process is relatively complicated and multistage, and its various aspects have been considered in detail in several works. For example, the thermochemical modeling of serpentinization was carried out in various geochemical settings in a wide temperature range with involvement of both fresh and sea water [5]. On land, the serpentinization process commonly involves groundwater at ambient temperature in conditions closed to the atmosphere. Hyperalkaline waters (a term accepted in the literature) are those with pH > 10. High pH in the most generalized form due to the mineral hydrolysis [4]:

$$4Mg_2SiO_4 + CaMgSi_2O_6 + 7H_2O \rightarrow 3Mg_3Si_2O_5(OH)_4 + Ca^{2+} + 2OH^-. \quad (2)$$

High pH of the discharged springs provides the absorption of atmospheric carbon dioxide and the subsequent deposition of calcium carbonates, sometimes dolomitized, so-called meteogenic travertines (for example, [6]). Such springs are almost always vis-

[a] *Institute of Volcanology and Seismology, Far East Branch, Russian Academy of Sciences, Petropavlovsk-Kamchatsky, 683000 Russia*
[b] *Sobolev Institute of Geology and Mineralogy, Siberian Branch, Russian Academy of Sciences, Novosibirsk, 630090 Russia*
[c] *Geological Institute, Russian Academy of Sciences, Moscow, 119017 Russia*
**e-mail: savelyev@kscnet.ru*

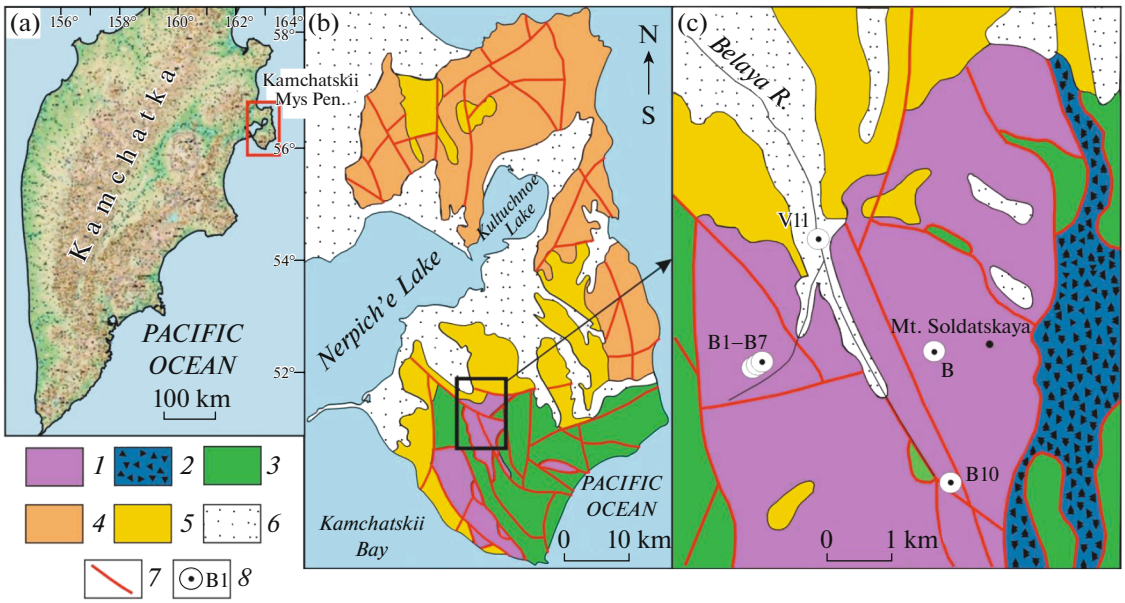

Fig. 1. (a) Kamchatsky Mys Peninsula on the map of Kamchatka; (b, c) tectonic map of the Kamchatsky Mys Peninsula and a simplified geological map of the study area after [15]. (*1*) Dunites and harzburgites of the Soldatskii massif (c), Cretaceous gabbro, ultrabasic rocks, and serpentinite mélange of the ophiolite assemblage (b); (*2*) serpentinite mélange; (*3*) Cretaceous volcanic–siliceous rocks of the Smaginskaya and Pikezhskaya formations; (*4*) Cretaceous–Paleogene rocks of the Kronotskii paleoarc; (*5*) Pliocene–Eopleistocene sea rocks of the Olkhovskaya Formation; (*6*) loose Quaternary rocks of various genesis; (*7*) main faults; (*8*) sampling sites. Point B indicates unanalyzed springs.

ible on the surface due to deposition of travertine. Travertines consist mainly of calcite and aragonite and are characterized by specific C and O isotopic compositions generally different from those of atmospheric CO_2 and, due to the kinetic fractionation effects, marked by an approximately linear trend on the $\delta^{18}O$ versus $\delta^{13}C$ plot (for example, [7] and references in this work). Due to the fact that meteogenic travertines are formed with involvement of atmospheric carbon dioxide, the radiogenic carbon content in them corresponds to the deposition time. Therefore, travertines from hyperalkaline springs can be used for geochronological purposes, if it is possible to analyze relatively thick layers of travertine deposits [6, 9].

The northernmost finding of such highly alkaline waters (approximately 58° N) is the Tablelands ultrabasic massif on Newfoundland Island (Canada) [10]. As far as we know, these waters have not been described in Russia. Alkaline waters are not mentioned even in the well-known monograph by Krainov et al. "Underground Water Geochemistry" [11], except for the Kola Peninsula borehole brines, the nature of which is not discussed.

Alkaline water springs (hereinafter, Soldatskie) with pH from 10.6 to 11.2 were found on the slopes of Mount Soldatskaya, within the Kamchatsky Mys Peninsula, during the field work in 2012 [12, 13] in Kamchatka. The field work in 2022 made it possible to carry out detailed studies and discover water springs with pH > 12. In this paper, we present the first study results for the chemical and isotopic compositions of water from eight springs, as well as data on the mineralogy and isotopic composition ($\delta^{13}C$ and $\delta^{18}O$) of associated travertines, including their radiocarbon age.

Ultrabasic rocks are relatively widespread in the southern part of the Kamchatsky Mys Peninsula; they form serpentinite mélange covers and zones with a thickness from a few to hundreds of meters [14]. The largest ultrabasic rock body with an area of about 70 km^2 is located in the upper reaches of the Belaya River, Mount Soldatskaya massif (Fig. 1). The erosion reaches 800 m in depth along the Belaya River valley. The Mount Soldatskaya peridotites occur as spinel harzburgites, lerzolites, and dunites. An important feature of ultrabasic rocks in the Mount Soldatskaya massif is uneven rock serpentinization from completely serpentinized varieties, sometimes transformed into serpentinite clays along tectonic zones, to almost fresh rocks with a serpentine content of no more than 0.5%.

All springs analyzed are discharged on rather steep slopes, forming small streams flowing down the slope. The stream channels are covered by light travertine sediments from pure white to yellow–brown. Figure 2 shows the location of the analyzed springs in the valley of the left tributary of the Belaya River at an absolute height of 480–580 m (230–330 m above the level of the Belaya River). All springs (B1–B7) are located on the side of the left bank; the uppermost ones, B5 and B6, are at a height of about 40 m above the valley bot-

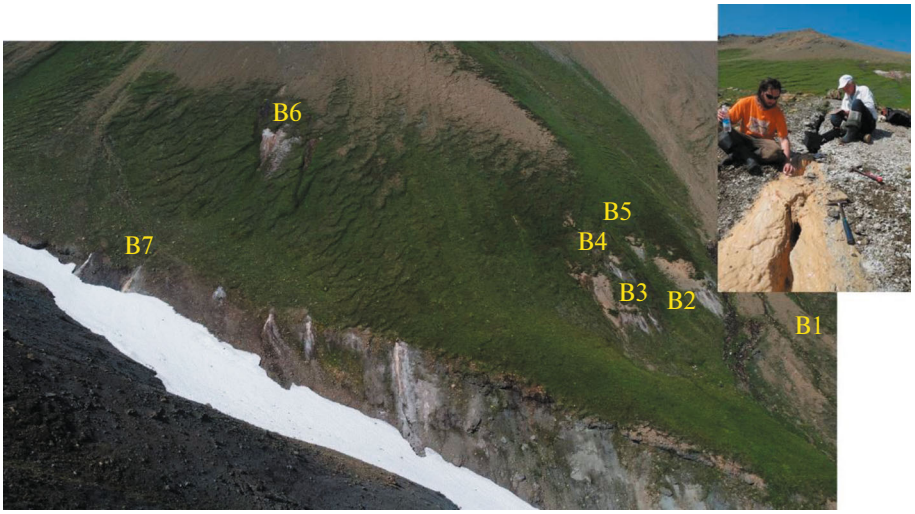

Fig. 2. Springs in the valley of the left tributary of the Belaya River. (Inset) Spring B7 discharged from a deep fracture with yellow travertine. Photo image by I. Savelev.

tom. At the edge of the coastal slope, the linear discharge of springs is marked by white travertine trails. Springs B1–B6 are small (approximately 20 × 20 cm^2 or less) pools in cemented rocks. Spring B7 is discharged from a tectonic fracture (Fig. 2, inset) apparently resulting from the travertine cover splitting during seismic movements. Spring B10 is located on the side of the alluvial terrace of the Belaya River at an altitude of about 10 m above the river level (385 m asl). Away from the spring, on the slope, there is a terrace that is a bedrock outcrop of highly serpentinized and carbonate-cemented fragments of ultrabasic rocks, which is likely a groundwater aquiclude. Spring B10 is distinguished by an extended (about 30 m) light brown travertine plume. No free gases were visually observed in any spring analyzed.

METHODS

The flow rates of the springs analyzed are very low (much lower than 1 l/s). The pH, temperature, and dissolved hydrogen concentration were measured with an YY-400 sensor (China) at the vents (Table 1). The chemical composition of the waters was determined in the laboratory by ion chromatography; alkalinity, by potentiometric titration. The isotope composition of the spring water (δD and $\delta^{18}O$) was analyzed with a Picarro L2140-i isotope analyzer at the Geological Institute, Russian Academy of Sciences. The results obtained for water are presented in δ units relative to the V-SMOW standard. The accuracy of determination of $\delta^{18}O$ and δD reached ±0.1‰ and ±1‰, respectively. The isotopic C and O compositions of travertines were determined at the Institute of Geology, National University of Mexico. The analysis was performed using the Gas Bench II option with a MAT 253 mass spectrometer (Thermo, Germany). CO_2 with a certified isotopic composition was used in the calibration. The samples and C-O-1 and NBS-19 standards were decomposed with 100% H_3PO_4 at 50°C. $\delta^{13}C$ and $\delta^{18}O$ are given in ppm (‰) relative to the V-PDB standard. The accuracy of determination of $\delta^{18}O$ and $\delta^{13}C$ is ±0.1‰.

X-ray diffraction analysis was also carried out with a Malvern Panalytical Empyrean diffractometer (45 kV, 40 mA, $4° < 2\theta < 80°$) at the Institute of Geology, National University of Mexico. The phases were identified using the HighScore v. 4.5 software.

The radiocarbon analysis was carried out in the BETA ANALYTIC Laboratory (United States) using the AMS (Accelerator Mass Spectrometer) method. The results were normalized to oxalic acid standard II (NIST SRM 4990C) and corrected with the help of the standard devoid of ^{14}C CO_2 (IAEA C-1).

The measurement accuracy was better than ±5‰ in terms of the current standard. The radiocarbon data are given in common ^{14}C ages according to [16]. The saturation indices were calculated using the SOLVEQ software with an improved thermodynamic database [17].

RESULTS AND DISCUSSION

Water composition. The chemical composition of waters from the springs analyzed is given in Table 2. Only two springs, B7 and B10, are characterized by a noticeable mineralization, clearly of sodium chloride composition. They are also distinguished by the highest pH values (11.6 and 12.3). The waters of other springs are extremely dilute, actually fresh, but with a high pH. All waters are almost sulfate-free with total $HCO_3^- + CO_3^{2-}$ of less than 250 mg/L.

Table 1. Coordinates of the springs, absolute elevations, and field characteristics. *S* is the specific conductivity

No.	Object	Latitude, N	Longitude, E	Asl, m	*T*, °C	pH	*S*, μS
B1	Spring	56°12.05′	162°54.02′	518	4.5	9.83	134
B2	– ” –	56°12.02′	162°53.82′	543	8.1	10.27	165
B3	– ” –	56°12.01′	162°53.81′	557	6.2	10.91	218
B4	– ” –	56°11.98′	162°53.75′	542	4.2	10.58	120
B5	– ” –	56°11.96′	162°53.73′	569	5.7	9.96	139
B7	– ” –	56°11.94′	162°53.80′	547	4.2	11.58	412
B10 top	– ” –	56°10.87′	162°56.39′	410	6.6	12.23	1264
B10 bottom	– ” –	56°10.87′	162°56.39′	400	8.1	12.01	1044
B11	River	56°12.74′	162°54.54′	244	4.3	8.86	103

Table 2. Chemical and isotopic compositions of waters in the Soldatskie springs

No.	B1	B2	B3	B4	B5	B7	B10.1	B10.2	B11
							Top	Bottom	River
T, °C	4.5	8.1	6.2	4.2	5.7	4.2	6.6	8.1	4.3
pH (field/lab)	9.1/9.83	9.61/10.27	10.53/10.91	10.21/10.58	–/9.96	11.5/11.58	12.1/12.3	–/11.91	–/8.86
Cl^-	6.8	6.3	10.3	6.1	6.1	32	162	139	2.4
SO_4^{2-}	1.1	1.0	1.4	2.1	0.40	0.56	0.40	0.65	1.3
Na^+	7.5	6.7	15.0	3.6	3.8	47	172	147	2.8
K^+	1.6	1.3	1.5	1.0	3.3	1.9	3.3	2.8	0.2
Ca^{2+}	3.4	8.3	13,8	7.8	6.7	2.0	2.8	4.6	8.7
Mg^{2+}	9.6	13.8	4.1	9.6	13.7	0.72	0.35	0.54	8.2
HCO_3^-	*56*	*63*	*28*	*32*	*73*	36	48	53	56
CO_3^{2-}	*11*	*36*	*65*	*33*	*19*	80	197	150	2
H_2(dis.)	0	0	0	0	0	0.032	0.61	0.32	0
δD ‰	–83.2		–86.9			–87.2	–85.8		–80.4
$\delta^{18}O$ ‰	–12.0		–12.8			–12.5	–12.9		–12.1

Concentrations, mg/L; dissolved hydrogen concentration, mmol/l. The numbers in italics are calculated HCO_3^- and CO_3^{2-} concentrations (see text).

The total of carbonate components in samples not subjected to the potentiometric analysis was determined from the ion balance. The $r = HCO_3^-/CO_3^{2-}$ ratio was calculated taking into account the $H^+ + CO_3^{2-} = HCO_3^-$ equilibrium, i.e., $r = 10^{(\log K - pH)}$, where *K* was an equilibrium constant. The calculation took into account the pH values determined in the laboratory. Mixing of fresh surface waters and sodium chloride waters of deeper horizons was observed in the Na–Cl coordinates (Fig. 3a). The nature of these Na–Cl waters is unclear, but most likely, they are related to Cretaceous marine sediments. Figures 3b and 3c show a relation among pH, Ca^{2+}/Mg^{2+}, and $HCO_3^- + CO_3^{2-}$. These graphs are very similar for almost all studied alkaline springs associated with ultrabasic rocks (for example, [8]). With an increase in alkalinity, the Mg concentration drops to the level of tens of μg/L as a result of brucite precipitation. Springs B1–B7 and B10 are supersaturated with respect to calcite, aragonite, talc, and serpentine (chrysotile), while a characteristic dependence on pH is observed with respect to brucite; brucite becomes supersaturated at pH > 11. The saturation indices are defined as the logarithm of the ratio of activity products in real solutions to theoretically activity products at given temperatures.

The isotopic composition points of the spring waters (Table 2), if plotted on the $\delta D - \delta^{18}O$ diagram, lie slightly above the Craig line, by about 6‰ in δD,

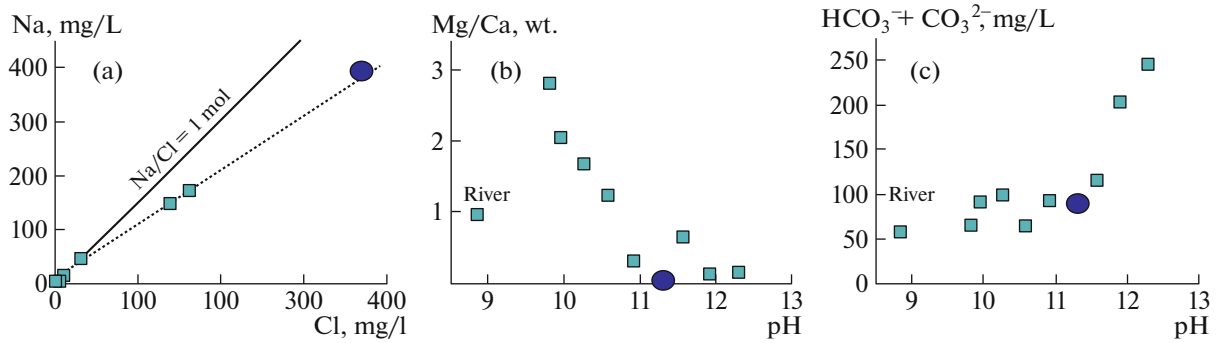

Fig. 3. (a) Mixing in coordinates of Na and Cl concentrations; (b, c) dependence of Mg/Ca (weight ratio) and carbonate total on pH. A blue symbol indicates the data from the report [13] (sample D1270); the analysis was made using water from spring B10.

but close to the regional line of meteoric waters proposed for the Kamchatka region in [18].

Dissolved hydrogen was found in springs B7 and B10. Moreover, in spring B10, its concentration turned out to be very high, about 0.6 mmol/L, i.e., half of the dissolved gas was hydrogen. The dissolved H_2 in spring B7 was about 20 times lower.

TRAVERTINE COMPOSITION

Mineralogy. Table 3 reports the X-ray diffraction and isotopic analysis data obtained for travertines from the springs analyzed. According to the X-ray diffraction analysis results, travertines are composed either mainly of calcite or aragonite; and in B4, also of magnesite. The variable polymorphism of carbonate sediments has been studied by many authors. In the case of meteogenic travertines, calcite is deposited at higher pH than aragonite (for example, [19]), but, in addition to pH, the solution supersaturation with respect to a particular mineral also plays an important role. It follows from this table that travertines of the highest alkaline spring B10 consist of 99% calcite, while travertines of springs B3, B4, and B7 are mainly composed of aragonite. However, in spring B5 with pH < 10, travertine mainly of calcite composition is also deposited. Hence, the relationship between solution pH and calcium carbonate polymorphism is ambiguous.

Isotopic C and O compositions of travertines. The isotopic C and O compositions of travertines are shown in Fig. 4 in $\delta^{18}O$ and $\delta^{13}C$ (VPDB) coordinates where the points of travertines of the most famous hyperalkaline waters of Oman, California, Northern Italy, and Newfoundland are added [7, 8, 10]. Travertines of the first three systems are characterized by a correlation between $\delta^{18}O$ and $\delta^{13}C$ in a wide range of values, from about 0‰ to –25‰ with a slope of about 1 : 1. The isotopically heavy endmember of this trend, similar to a mixing trend, is atmospheric carbon dioxide, while the most isotopically lightened members reach values characteristic of organic carbon. This general trend, as shown in recent works, is not the result of mixing, but the product of kinetic isotope fractionation during carbonate deposition due to dissolution of atmospheric CO_2 in water with high pH [7, 8]. Temperatures of the springs of the first three systems located in snowless regions with a warm climate are above 20°C, on average; the Oman springs have a temperature of above 30°C. However, the points of Soldatskie travertines evidently fall out of this trend: they occur much to the right of it and do not correlate with each other. Points for the Newfoundland travertines are plotted close to our points [10]. Newfoundland springs have temperatures of 8–15°C; Soldatskie springs, from 4 to 8°C. It is possible that the observed effect is somehow related to the spring discharge and carbonate deposition temperature. A much larger set of samples, of both water and travertine, needs to be analyzed to try to understand these patterns.

Table 3. X-ray diffraction data (wt %), isotope composition ($\delta^{13}C$ and $\delta^{18}O$), and ^{14}C age of travertines

No.	pH	Aragonite	Calcite	Magnesite	$\delta^{13}C$ VPDB	$\delta^{18}O$ VPDB	^{14}C age, year
B3	10.53	91.9	0	0	–12.4	–9.2	–
B4	10.21	62.4	6.6	31	–2.2	–9.5	–
B5	9.96	0	97.8	0	–5.7	–10.4	–
B7	11.5	95.2	4.8	0	–10.7	–9.5	1180 ± 30
B10 top	12.1	0	99.8	0	–17.7	–17.0	114 ± 0.4
B10 bottom	11.9	–	–	–	–16.9	–16.2	104 ± 0.4

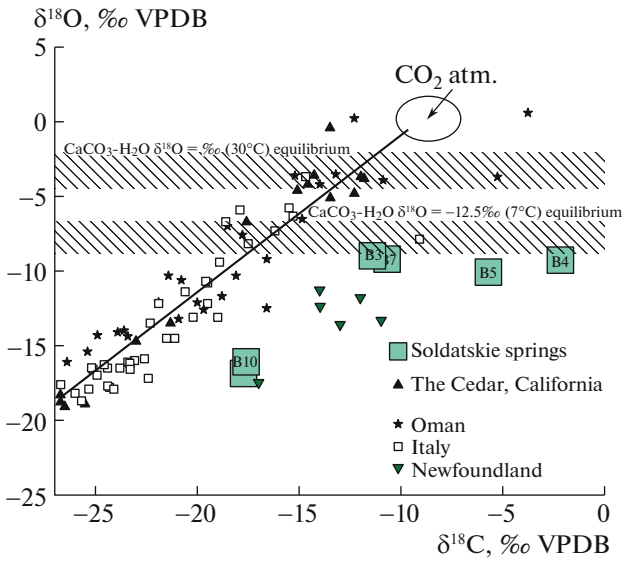

Fig. 4. Isotopic composition of travertines from the Soldatskie springs. Data on the best-known alkaline systems in Oman, California (the Cedar), Northern Italy, and Newfoundland Tablelands travertines. The first three systems form a general trend, while the composition points of the Soldatskie springs and Newfoundland travertines are shifted to the right [7, 8, 10]. Shaded fields are calculated values of calcium carbonate in equilibrium with water with different oxygen isotopic compositions at different temperatures (see text).

It also should be noted that a certain limit for the O isotope composition of travertines, in both the Soldatskie springs and the alkaline waters of Oman and California, is the zone of compositions close to $\delta^{18}O$ values determined from the isotopic equilibrium between water and carbonate (calcite, aragonite, or dolomite). The graphs show these zones for the Oman springs with water $\delta^{18}O$ of about 0‰ (VSMOW) and an average spring temperature of 30°C, as well as for the studied springs with water $\delta^{18}O$ of −12.5‰ (VSMOW) and an average temperature of 7°C. These zones are shown by the shaded field in Fig. 4; the equations for equilibrium factors of fractionation of oxygen isotopes between carbonates and water given in [20] were used in the calculation.

Travertine age. Travertines of spring B10 with pH > 12 turned out to be almost recent (Table 3), and the sediment age at the spring outlet and 30 m below, in the stream channel, is approximately the same (about 100 years). The sample chosen to determine the age of spring B7 with pH 11.5 was taken in the fracture niche which the spring water flows along (Fig. 2, inset). It was something like a small stalactite of about 2 cm in size. It turned out to be much older (1180 years). In any case, these age determinations are indicative of the fact that the current carbon content is above 90% in travertines B7 and B10. In other words, only atmospheric CO_2 can be the source of this carbon. Perhaps it should be noted that $^{14}C/^{12}C$ in recent atmospheric CO_2 almost approached this ratio at the pre-bomb (before 1950) CO_2 level [16].

CONCLUSIONS

A detailed description of hyperalkaline springs (pH > 10) discharged within the ultrabasic massif of Mount Soldatskaya in the Kamchatsky Mys Peninsula is given for the first time.

The chemical composition of the spring waters and the dependence of Ca^{2+}/Mg^{2+} and the alkalinity ($HCO_3^- + CO_3^{2-}$) on pH are indicative of the fact that these waters were formed due to the modern serpentinization of ultrabasic rocks.

Dissolved hydrogen with a concentration of approximately 0.6 mmol/l was detected in the spring waters with the highest alkaline levels (pH 12.3).

The isotope composition ($\delta^{13}C$ and $\delta^{18}O$) of carbonate deposits (travertines) deposited from these spring waters differs from the known trend established for "meteogenic" travertines, possibly due to the extremely low temperatures of the springs (4–8°C).

The age of travertine determined by the radiocarbon method is close to recent (100–1000 years).

ACKNOWLEDGMENTS

We are grateful to E. Voloshina, T. Pi-Puig, F. Otero, and A. Ermakov for analytical works, and also to N. Nekrylov for help in the field work. Highly professional remarks given by E.O. Dubinina made it possible to improve this paper significantly.

FUNDING

This study was supported by the Russian Science Foundation, grant no. 22-27-00029.

CONFLICT OF INTEREST

The authors declare that they have no conflicts of interest.

REFERENCES

1. I. Barnes, V. Lamarche, Jr., and G. Himmelberg, Science **156**, 830–832 (1967).
2. V. Chavagnac, C. Monnin, G. Ceuleneer, C. Boulart, and G. Hoareau, Geochem., Geophys. Geosyst. **14** (7), 2496–2522 (2013).
3. E. Dubinina, I. Chernyshew, N. Bortnikov, A. Lein, A. Sagalevich, Y. Gol'zman, E. Bairova, and A. Mokhov, Geochem. Int. **45**, 1131–1143 (2007).
4. A. N. Paukert, J. M. Matter, P. B. Kelemen, E. L. Shock, and J. R. Havig, Chem. Geol. **330**, 86–100 (2012).
5. J. L. Palandri and M. H. Reed, Geochim. Cosmochim. Acta **68** (5), 1115–1133 (2004).
6. A. Pentecost, *Travertine* (Springer-Verlag, Berlin, 2005).
7. J. N. Christensen, J. M. Watkins, L. S. Devriendt, D. J. DePaolo, M. E. Conrad, M. Voltolini, W. Yang, and W. Dong, Geochim. Cosmochim. Acta **301**, 91–115 (2021).
8. E. M. Schwarzenbach, S. O. Lang, G. L. Fruh-Green, M. Lilley, S. M. Bernasconi, and S. Mehay, Lithos **177**, 226–244 (2012).
9. L. Ternieten, G. L. Früh-Green, and S. M. Bernasconi, J. Geophys. Res.: Solid Earth **126**, e2021JB022712 (2021). https://doi.org/10.1029/2021JB0227
10. N. Szponar, W. J. Brazelton, M. O. Schrenk, D. M. Bower, A. Steele, and P. L. Morrill, Geochemistry of a continental site of serpentinization, the Tablelands Ophiolite, Gros Morne National Park: A Mars analogue, Icarus **224** (2), 286–296 (2012). https://doi.org/10.1016/j.icarus.2012.07.004
11. S. R. Krainov, B. N. Ryzhenko, and V. M. Shvets, *Underground Water Geochemistry. Theoretical, Applied, and Ecological Aspects* (Nauka, Moscow, 2004) [in Russian].
12. D. P. Savelev, R. M. Novakov, and R. I. Cherkashin, Vestn. Kamchatskoi Reg. Assots. Uchebn.-Nauchn. Tsentra Nauki Zemle, No. 2 (Iss. 24), 7–11 (2014).
13. R. M. Novakov, D. P. Savelev, T. P. Belova, and S. V. Palamar', in *Proc. Conf. Dedicated to Volcanologist Day "Volcanism and Related Processes"* (Inst. Volcanol. Seismol. Far-Eastern Branch Russ. Acad. Sci., Petropavlovsk-Kamchatsky, 2014), pp. 97–103 [in Russian].
14. M. Yu. Khotin and M. N. Shapiro, Geotectonics **40** (4), 297–321 (2006).
15. M. E. Boyarinova, N. A. Veshnyakov, A. G. Korkin, and D. P. Savelev, *The 1 : 200 000 State Geological Map of the Russian Federation, 2nd ed., Ser. Eastern Kamchatka, Sheet No. O-58-XXVI, XXXI, XXXII (Ust'-Kamchatsk), Explanatory Note* (Kartfabr. Karpinsky Russ. Geol. Res. Inst., St. Petersburg, 2007).
16. P. J. Reimer, T. A. Brown, and W. Reimer Ron, Radiocarbon **46** (1), 1111–1150 (2004).
17. M. H. Reed and N. F. Spycher, Geochim. Cosmochim. Acta **48**, 1479–1492 (1984).
18. A. L. Cheshko and A. D. Esikov, Vodn. Resur., No. 6, 34–43 (1990).
19. B. Jones, Sediment. Geol. **353**, 64–75 (2017).
20. J. Horita, Geochim. Cosmochim. Acta **129**, 111–124 (2014).

Translated by E. Maslennikova